Geothermics 122 (2024) 103081

Contents lists available at ScienceDirect

Geothermics

journal homepage: www.elsevier.com/locate/geothermics

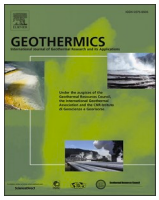

Probabilistic assessment of deep geothermal resources in the Cornubian Batholith and their development in Cornwall and Devon, United Kingdom

Aysegul Turan [a,*], Christopher S Brown [b], Robin Shail [c], Ingo Sass [a,d,e]

[a] Geothermal Science and Technology, Institute of Applied Geosciences, Technical University of Darmstadt, Schnittspahnstrasse 9, 64287 Darmstadt, Germany
[b] James Watt School of Engineering, University of Glasgow, Glasgow, G12 8QQ
[c] Camborne School of Mines, Department of Earth and Environmental Science, University of Exeter, Penryn Campus, Penryn, Cornwall, TR10 9FE, UK
[d] GFZ German Research Centre for Geosciences, Section 4.8: Geoenergy, Telegrafenberg, 14473 Potsdam, Germany
[e] Graduate School of Excellence Energy Science and Engineering, Technical University of Darmstadt, 64287 Darmstadt, Germany

ARTICLE INFO

Keywords:
Cornubian Batholith
Geothermal resource assessment
Monte Carlo simulation
Enhanced geothermal system
Hot dry rock

ABSTRACT

Geothermal energy could play a pivotal role in decarbonisation as it can provide clean, constant base-load energy which is weather independent. With a growing demand for clean energy and improved energy security, geothermal resources must be quantified to reduce exploration risk. This study aims to quantify the untapped resource-potential of the Cornubian Batholith as a geothermal resource for power generation and direct heat use. Recent field work, laboratory measurements and petrophysical characterization provides a newly compiled dataset which is inclusive of subsurface samples taken from the production well of the United Downs Deep Geothermal Power Project. Deterministic and probabilistic calculations are undertaken to evaluate the: total heat in place, recoverable resource, technical potential and potential carbon savings. The Cornubian Batholith is considered a petrothermal system which may require stimulation as an enhanced geothermal system. This study shows the batholith has significant heat stored of 8988 EJ (P50), corresponding to 366 EJ recoverable and a technical potential of 556 GW_{th}. When evaluating the potential for power generation (i.e., electricity) the P50 is 31 GW_e. The total carbon savings when generating electricity (P50) equates to 106 Mt.

1. Introduction

Globally, renewable energy sources must be considered to reduce carbon emissions and improve energy security (e.g., Hache, 2018). There are two major legislative drivers binding the UK to meet 2050 net-zero carbon emissions targets (BEIS, 2019): i) By the year 2030, it is anticipated that 95% of the electricity in Britain could come from low-carbon sources. By 2035, electricity systems are expected to be fully decarbonized, contingent upon security of supply (Department for Energy Security and Net Zero, Prime Minister's Office, and Department for Business, Energy & Industrial Strategy, 2022), ii) the 2008 UK Climate Change Bill where present and future governments are obliged to follow publicly announced CO_2 reduction plans. This requires all newly built houses after 2025 to have low carbon heating systems (Batchelor et al., 2020). Therefore, considering the UK's goals related to energy production, the exploitation of alternative energy sources, such as geothermal, are essential.

Geothermal energy can provide a low-carbon energy source and is often overlooked; however, shallow-to-deep geothermal resources are widely distributed across the UK (Downing and Gray, 1986; Busby et al., 2014; Busby and Terrington, 2017; Watson et al., 2019; Abesser et al., 2023a). Yet, the geothermal sector is in its infancy as only one deep (>500 m) hot sedimentary aquifer has been exploited in Southampton, since the 1970s, which recently ceased production (e.g., Barker et al., 2000; Younger et al., 2012; Abesser et al., 2023a), and only one open-loop deep hot dry rock system is in the late stages of development at the United Downs Project in Cornwall (e.g., Ledingham et al., 2019; Paulillo et al., 2020; Reinecker et al., 2021). There is also heat being extracted through a closed-loop coaxial deep borehole heat exchanger from the Eden Project, also in Cornwall (Hueber, 2023; Abesser et al., 2023a), while other closed-loop systems are being developed around the UK (e.g., Brown and Howell, 2023; Brown et al., 2023), typically using the coaxial configuration at depth for improved thermal and hydraulic efficiency (Brown et al., 2024). In contrast, the shallow geothermal sector has many developments, with open- and closed-loop systems across the UK, and it is estimated there are over 48,000 ground source

* Corresponding author.
E-mail address: turan@geo.tu-darmstadt.de (A. Turan).

https://doi.org/10.1016/j.geothermics.2024.103081
Received 3 February 2024; Received in revised form 20 May 2024; Accepted 10 June 2024
Available online 26 June 2024

heat pump installations with a capacity of 903 MW_{th} (Abesser et al., 2023b).

Cornwall Council (Southwest UK) has set a challenging target of reaching carbon neutrality by 2030 (IPCC, 2021) owing to its high geothermal potential. A large part of the region has high heat flows of up to 117 mW/m^2, more than twice the UK average of 55 mW/m^2, arising from the radioactive decay of elements U, Th and K within the Cornubian Batholith (Beamish and Busby, 2016). In Cornwall, the climate is oceanic with an annual precipitation of 905.71 mm and the annual average temperature is 14.18 °C (Met Office, n.d.). Considering the time with an ambient temperature below 18 °C, heating is needed for eight months of the year.

This study investigates the geothermal potential of the Cornubian Batholith in Cornwall and Devon (Fig. 1). Past estimates of the total heat in place used deterministic methods (Downing and Gray, 1986; Busby and Terrington, 2017), whilst in this study probabilistic analysis was conducted to provide uncertainty quantification. Two scenarios were considered, including direct (i.e., generation of heat that can be used for district heating, heating of greenhouses, agricultural drying, heating of road and side-walks in winter) and indirect utilization (i.e., electricity generation) of geothermal resource associated with the Cornubian Batholith as a petrothermal system, following the criteria of Breede et al. (2015). New data has been acquired, providing better petrophysical and geometrical constraints of the granite. After fieldwork and sampling in June 2019 (Fig. 2), laboratory-scale petrophysical, petrographical and geochemical characterization was performed on outcrop samples across Cornwall and Devon, plus drill cuttings (Turan et al., 2024) and sidewall cores (Stark et al., 2021) from the production well (UD-1) at the United Downs Deep Geothermal Power project. The volumetric method was applied, using the newly acquired data, to calculate thermal energy content and to estimate how much energy is recoverable to generate electric and thermal power (Muffler and Cataldi, 1978). A probabilistic study, using Monte Carlo simulation, was carried out to account for the uncertainty associated with reservoir characteristics. Sustainability attributes, including carbon emissions, were analysed assuming the currently dominant electrical and thermal source. The work presented may inform further development of deep geothermal energy across Cornwall and Devon, and so contribute to increased decarbonisation and reduced energy security issues; it complements recent national-to-local deep resource estimations (e.g., Busby and Terrington, 2017; Brown, 2022, 2023; Abesser et al., 2023a; Jones et al., 2023)

2. Geological and thermal overview

Cornwall and Devon represent a Variscan massif, largely comprising Early Devonian to late Carboniferous sedimentary and volcanic successions that underwent deformation and low-grade regional metamorphism during Carboniferous Variscan continent-continent collision (Leveridge and Hartley, 2006; Shail and Leveridge, 2009). Post-collisional extension initiated in the late Carboniferous, persisted throughout the Early Permian and was associated with mantle and crustal melting that resulted in the generation and emplacement of the Cornubian Batholith over 20 myr *c.* 293–274 Ma (e.g., Chen et al., 1993; Simons et al., 2016; Shail and Simons, 2023). The batholith is hosted by the Devonian-Carboniferous successions and comprises six major plutons that crop out from the Isles of Scilly, offshore to the west, to Dartmoor in the east. As highlighted in Fig. 1, the surface expression of the Cornubian Batholith stretches approximately 250 km in a west-east direction and 40 km in a north-south direction (Taylor, 2007), including six granitic plutons, from west to east: Isles of Scilly (120 km^2), Land's End (190 km^2), Carnmenellis (135 km^2), St Austell (85 km^2), Bodmin Moor (220 km^2), and Dartmoor (650 km^2). Five principal granite types have been recognised in near-surface exposures (Fig. 2): G1 (two-mica granite), G2 (muscovite granite), G3 (biotite granite), G4 (tourmaline granite) and G5 (topaz granite) (Simons et al., 2016). All are peraluminous; G1-G4 are monzogranites or syenogranites whilst G5 are alkali feldspar granites (Simons et al., 2016). The granites and their Devonian-Carboniferous host rocks are cut by a series of broadly NNW-SSE striking, steeply-dipping, 'cross-course' fault zones that are the present focus of deep geothermal exploration. The Porthtowan Fault Zone has been targeted at the United Downs Deep Geothermal site (e.g., Reinecker et al., 2021) and the Great Cross-course at the Eden Geothermal site (e.g., Huebert, 2023). Cross-course fault zones have a complex evolution involving multiple episodes of reactivation, including as extensional faults during Mid-Triassic rifting (e.g., Shail and Alexander, 1997) and as strike-slip faults during Cenozoic intraplate shortening (e.g., Dearman, 1963). The damage zones around the principal NW–SE faults have a width of 100–200 m and contain more frequent cross-cutting features that may enhance connectivity of the fracture network (Yeomans et al., 2022).

Water inflow into metal mines in Cornwall, prior to their abandonment in the 1980s-1990s, evidenced the permeability of the fracture network within the granite. Certain cross-course flows discharged consistently for over three decades, indicating the presence of a substantial reservoirs of saline thermal water at significant depths (e.g., Edmunds et al. 1984).The Cornubian Batholith is continuous at depth based on the gravity anomaly data (Bott et al., 1958) and has an estimated volume of 76,367 ± 17,286 km^3 (Watts et al. 2024). Heat generation is variable, depending on the U, Th and K content, which were primarily controlled by source rock heterogeneities and melting

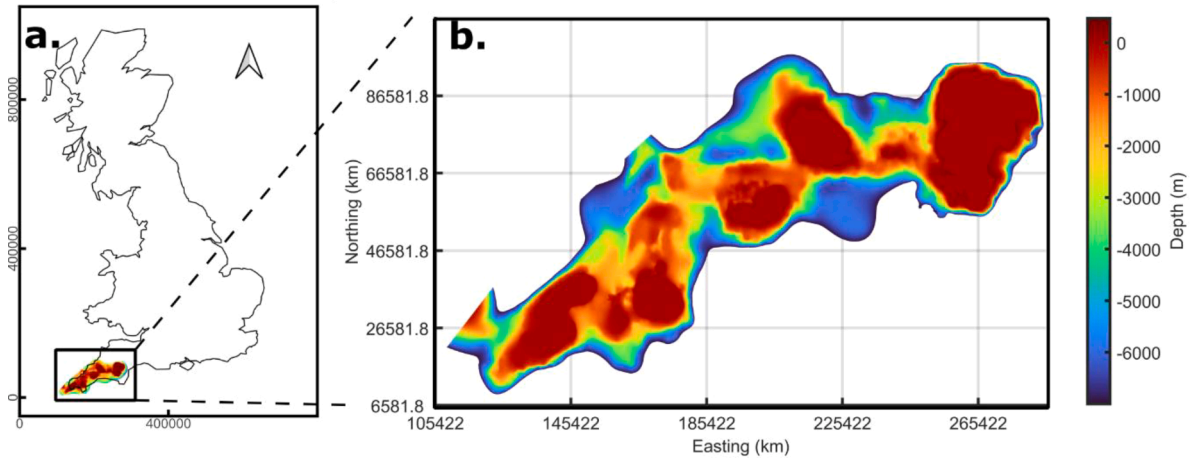

Fig. 1. (a) Location of the UK and (b) study area with depth to top surface of the granite. Derived from Lithoframe data – Filled_TopGranite and TopGranite_CHPM_40 m scale BGS Digital Data under Licence No. 2023/108 British Geological Survey © and Database Right UKRI. All rights reserved.

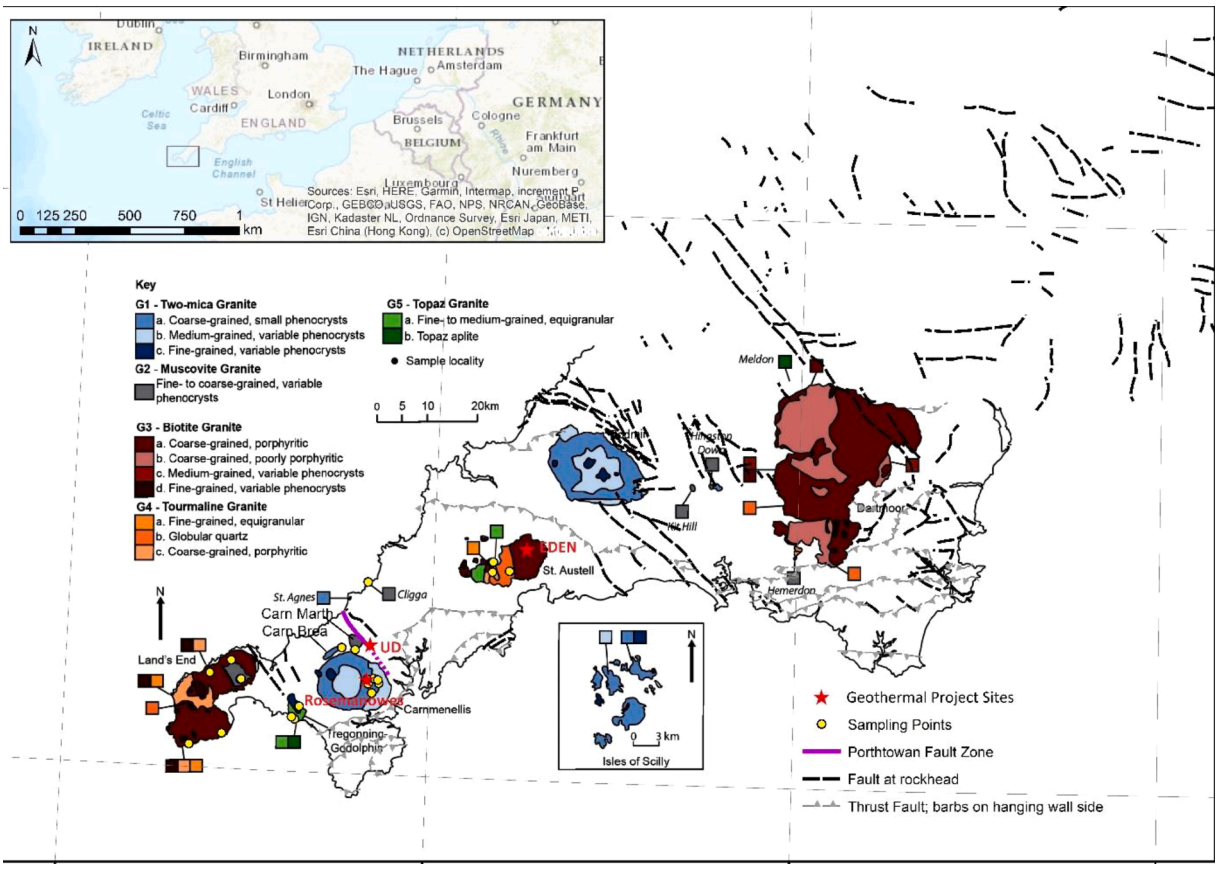

Fig. 2. Geological map of MEET sampling points (shown as yellow dots) with respect to location of geothermal projects (shown as red stars) (modified after geology map: BGS Onshore Geoindex (2019) and granite classification: Simons et al. 2016).

temperature (Dalby, 2023). The work of Beamish and Busby (2016) predicted temperatures in the granites at 5 km depth to be 206 °C (Land's End), 200 °C (Carnmenellis, which hosts the United Downs Geothermal project), 221 °C (St. Austell, which hosts Eden Geothermal project), 200 °C (Bodmin Moor), and 185 °C (Dartmoor).

3. Methods

Numerical investigation was undertaken using the classic volumetric heat in place method (e.g., Muffler and Cataldi, 1978) and unique carbon savings assessments (e.g., Turan et al., 2021). The volumetric heat calculations are commonly used internationally to give an indication of geothermal resources (e.g., Alimonti et al., 2021; Barcelona et al., 2021). The heat in place was determined using the modified method (Brown, 2022) for more detailed geometrical constraints, based on depth maps of the granitic resource and a base cut-off of 7 km in Southwest England.

3.1. Geothermal resource assessment

Deterministic and probabilistic assessment was undertaken using the volumetric method (Muffler and Cataldi, 1978). The geothermal resource or heat in place is determined as a function of the difference in rejection temperature and reservoir temperature, and bulk volumetric heat capacity of the rock and saturated fluid. Two separate analyses were conducted, determining the overall resource when heat is extracted, with rejection temperatures set to ambient conditions, and also for electricity generation only when the reservoir temperature must be in excess of 100 °C and a rejection temperature of 60 °C was used.

The Cornubian Batholith was divided into a series of grid blocks based on the depth map to the top of the granite, while the base of the resource was fixed at 7 km, which is assumed to be the maximum targeted drilling depth. This is similar to other work determining the geothermal resources of UK granites (e.g., Downing and Gray, 1986; Brown, 2022). There is ambiguity in the thickness of the Cornubian Batholith. Willis-Richards and Jackson (1989) suggest a thickness of 14 km, while Brooks et al. (1984) suggest the base could be around 8 km. A recent detailed 3D re-appraisal of the gravity data has indicated a minimum thickness of 10 km along the length of the batholith (Watts et al. 2024). The sum of the stored heat in place (E_{hip}) in each grid block was then calculated. There is further adaptation in this study of the method of Brown (2022) as the volume of the fluid stored in fracture porosity is also considered:

$$E_{hip} = \sum_{1}^{n} V.(\varnothing.\rho_f.c_f + (1-\varnothing).\rho_r.c_r).(T_n - T_r) \quad (1)$$

where V is the volume of a node, ρ is the density, c is the specific heat capacity, T_n is the temperature of the specific grid block located within the granite, T_r is the rejection temperature and n is the number of grid blocks of the granite. The subscripts $f$and r within the volumetric heat capacity term are for the fluid and rock, respectively.

The useable or recoverable thermal energy (E_r) can be calculated as a function of the recovery factor (R):

$$E_r = R.E_{hip} \quad (2)$$

The technical potential can be calculated over the lifetime of a system:

$$TP = \frac{E_{hip}.R.\eta}{t_{30}.LF} \quad (3)$$

Where η is the conversion efficiency of the plant, t is the lifetime of the system (30 years as suggested in Garg and Combs, 2015) and LF is

the load factor. It is worth noting, however, that if the resource is operated sustainably, it could be operated for far longer (Sanyal, 2005). The model uses an orthogonal mesh with uniform grid blocks of 40 by 40 m laterally, while the thickness of each grid block varies with the thickness of the granite. The average temperature is calculated to increase linearly with depth, with a surface temperature of 10 °C assumed.

3.2. Carbon savings assessment

Heating, as one of the highest carbon emitters, representing 37% of the UK total emissions (Department for Business, Energy, and Industrial Strategy, 2019) is the sector that needs significant decarbonisation to achieve 2050 net zero emission target. The record level of oil and gas prices caused by the recovery from the Covid-19 pandemic, and Russia-Ukraine war (Pearson and Watson, 2023) is another motivation to evaluate low-carbon, domestic and base load sources of energy such as geothermal. In this study, the impact of producing heat or electricity from the Cornubian Batholith is examined in terms of annual amount of saved CO_2 emissions by exploiting the geothermal system in Cornwall and Devon, rather than natural gas.

The following assumptions were made: i) complete combustion is assumed to occur, ii) natural gas is 100% composed of methane (CH_4), iii) 1 joule= 0.239 cal. combustion of 1 m^3 natural gas yields 8250 kcal energy (Çengel, 2020; Meşin and Karakaya, 2023), iv) density of natural gas is equal to 0.68 kg/m^3 (Eswara et al. 2013), v) all the CO_2 would be released directly into the atmosphere without any capture, vi) natural gas' combustion reaction with oxygen is as follows: $CH_4+2O_2 \rightarrow CO_2+2H_2O$, and vii) the efficiency of the natural gas cycle power plant, described by the thermal efficiency (η_{th}), is 50%, indicating that 50% of the heat input is converted into useful work output. The governing equation for thermal efficiency in the context of a power plant is:

$$\eta th = \frac{Useful\ work\ Output}{Heat\ Input} \tag{4}$$

For a natural gas cycle power plant, the thermal efficiency can be further expressed in terms of the key temperatures in the cycle, such as the high-temperature T_{hot} and low-temperature T_{cold}:

$$\eta th = 1 - \frac{Tcold}{Thot} \tag{5}$$

This equation is derived from the Carnot efficiency, which represents the maximum theoretical efficiency of a heat engine operating between two temperature reservoirs.

3.3. Parameterisation

In the model, the following parameters are defined with triangular probability density functions: porosity, recovery factor, geothermal gradient and fluid density. Conversely, the rock density parameter is defined with a uniform probability density function. All other input parameters (specific heat capacity of rock, specific heat capacity of fluid, reject temperature, project lifetime, load factor, and conversion factor) are defined as constant values. Several parameters were considered with the probability distributions (Figs. 4 and 5 for the different simulations, respectively) determined from new data (Table 1). The data publication associated with the parameterisation in this study (Turan et al., 2024) contains the raw outcrop data of the parameters (grain density and bulk density for the calculation of porosity, thermal conductivity and thermal diffusivity for the calculation of specific heat capacity). This data is also in line with drill cuttings and sidewall cores and is summarized in Table A1 in the Appendix.

Previous resource assessment studies (Yamanlar et al. 2020; Korkmaz et al. 2014; Arkan and Parlaktuna, 2005) have suggested porosity is best represented by triangular probability distribution frequency (PDF). Porosities were calculated, for 187 cores from outcrop analogue samples, based on the results of grain and bulk density measurements, conducted using a helium pycnometer and a powder pycnometer, respectively. Grain density was determined in a gas expansion pycnometer (AccuPyc II 1340) by applying helium as displacement fluid. The manufacturer of the equipment states that the accuracy for grain density measurements is 0.02% (Micromeritics, 2023). Bulk density measurements are made with an envelope density analyser (GeoPyc 1360). A well-sorted, fine-grained powder (Dry Flo) is utilized as displacement material to determine the bulk volume of the specimen. The bulk volume and weight of the specimen are used to calculate the bulk density, which is then combined with the grain density to determine the specimen's gas-effective porosity. The manufacturer specifies that the accuracy of this process is within 1.1% (Micromeritics, 1998). The minimum and maximum porosity values established from new data are 0.03% and 19%, respectively. The peak (most likely i.e., median) value is 1.05% where the standard deviation is 2.54, Quartile 25% is 1.00% and Quartile 75% is 2.53%

Reservoir thickness varies depending on each 40 × 40 m grid cell of the geometrical metadata, with the thickness calculated from the surface top to 7 km depth. Rock temperature was determined using a linear extrapolation based on the geothermal gradient to determine the average temperature of each model node (see Fig. 3 for peak temperature gradient at top surface). Note the temperature of the rock node is taken as the mid-point between the granite top and 7 km base. The geothermal gradient is measured at United Downs Deep Geothermal Power project site as 37.2 °C/km (Somma et al. 2021). Considering granite related temperatures at 5 km depth in the Cornubian Batholith are estimated to be in the range of ≈ 185 °C– 220 °C by Beamish and Busby, 2016 where the temperature was estimated as 200 °C at Carnmenelis granite that hosts United Downs project, minimum, peak and maximum values of geothermal gradient are assigned as 31, 35 and 40

Table 1
Summary of parameters modelled. *Reject temperature varied for different analysis (total heat use and electricity generation only). The asterisk indicates electricity generation. Also note the rock density used for deterministic analysis was 2650 kg/m^3. **Lithoframe data – Filled_TopGranite and TopGranite_CHPM_40 m scale BGS Digital Data under Licence No. 2023/108 British Geological Survey © and Database Right UKRI.

Parameter	Min	Peak	Max	Unit	Distribution	Reference
Reject Temperature		10 60*		°C	Constant	
Load Factor		0.66 0.96*			Constant	Garg and Combs, 2015
Conversion Factor		0.95 0.12*			Constant	
Fluid Heat Capacity		4400		J/(kg·K)	Constant	
Porosity	0.03	1.05	19.02	%	Triangular	Own data
Reservoir Thickness		Variable		km	n/a	BGS Data
Reservoir Area		6019		km^2	Variable	BGS Data**
Recovery Factor	0.2	2	10	%	Triangular	
Geothermal Gradient	31	35	4 0	°C/km	Triangular	Batchelor (1982), Gluyas et al. (2018), Ledingham et al. (2019), Somma et al. (2021)
Rock Density	2603		2796	kg/m^3	Uniform	Own data
Fluid Density	900	1000	1100	kg/m^3	Triangular	Batzle and Wang (1992)
Specific Heat Capacity		772		J/(kg·K)	Constant	Own data

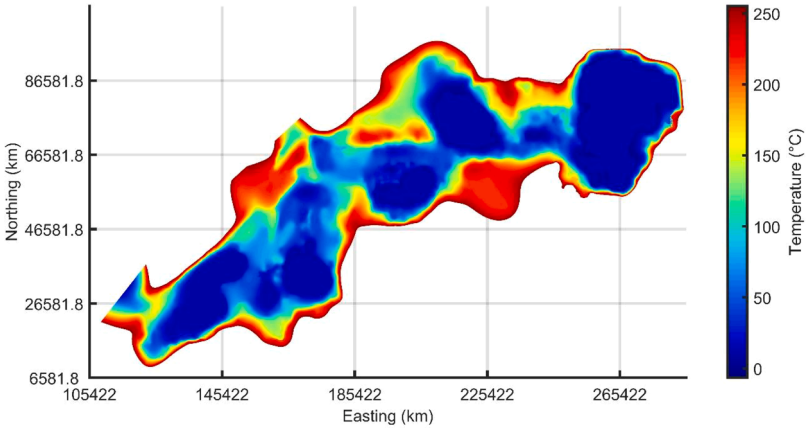

Fig. 3. Temperature at the top surface of the granite calculated using a linear geothermal gradient of 35 °C/km. Derived from Lithoframe data surfaces – Filled_-TopGranite and TopGranite_CHPM_40 m scale BGS Digital Data under Licence No. 2023/108 British Geological Survey © and Database Right UKRI. All rights reserved.

°C/km in the model.

Saline groundwaters (up to 19,310 ppm total dissolved solid) were identified in tin mines in the Carnmenellis granite at depths up to 800 m (Edmunds et al. 1984). Using salinity-temperature-pressure-density relationship, a triangular distribution was defined with values of 900 to 1100 kg/m^3 after Batzle and Wang (1992). Based upon the data available rock density, measured on 203 cores, was ascribed uniform distribution within the range of 2603 kg/m^3 and 2796 kg/m^3.

The recovery factor represents the amount of heat that is advected by fluid from the subsurface to the surface. It might rise as cooling cracks form from continuous heat extraction, enhancing permeability and allowing more fluid circulation for heat extraction, or through the chemical dissolution of fracture fillings. Conversely, permeability could decrease due to mineral deposition in open fractures. To cover the change in recovery factor with time and associated uncertainty, the recovery factor is represented by triangular PDF, which is in line with other resource estimation studies (Muffler 1978; Avşar, 2011; Arkan and Parlaktuna, 2005). It differs from hydrothermal systems, which can often have recovery factors of up to 25% (Tester et al. 2006), whilst enhanced geothermal systems are often far lower. Grant (2016) reported recovery factors of only 0.2–2% for the research EGS sites. Recent analyses of data from fractured geothermal reservoirs suggest that recovery factor is around 10%, with a range spanning from about 5% to 20% (Williams, 2007). Thus, the distribution is to the lower end of recovery factors. Minimum, peak and maximum values are assigned as 0.2%, 2% and 10%.

All other parameters were assigned constant values as there is low variation in specific heat capacity, and the reject temperature was fixed. Specific heat capacity of the rock was calculated based on the thermal conductivity, thermal diffusivity and bulk density measurements conducted on 195 cores, presented in Turan et al. (2024) through the formula, typically attributed to Fourier's law of heat conduction:

$$s = \frac{TC}{(TD\ X\ d)} \tag{6}$$

Where s is specific heat capacity (J kg^{-1} K^{-1}), TC is thermal conductivity (W m^{-1} K^{-1}), TD is thermal diffusivity (m^2 s^{-1}) and d is bulk density (kg m^{-3}). Specific heat capacity of fluid is taken as 4400 J/(kg·K) that corresponds to the typical reservoir temperature of the granite. Note the reject temperatures of the model was set as 10 °C for the total heat use analysis and as 60 °C for electricity generation to reduce the risk of scaling in the wellbore. For power generation a model cut-off and minimal temperature was set as 100 °C, otherwise efficiency of the power plant is below c.10% and unlikely to be economic. PDFs for the two simulations of total heat use and electricity generation are presented in Figs. 4 and 5, respectively.

4. Results

4.1. Deterministic assessment

A deterministic analysis was conducted to make an initial assessment on the geothermal potential of the Cornubian Batholith using 'peak' values assigned in Table 1. This was using two assumptions: i) The first was all heat in place could be extracted and utilised before reinjection. Therefore, the rejection and minimum temperature was set at 10 °C, the efficiency was 95%, and the load factor was 0.66 as much of the energy would be used for district heating. ii) The second was assuming resources over temperatures of 100 °C within the modelled domain to enable power generation, rather than that of the total resource. Rejection temperature was limited to 60 °C, efficiency based of plant conversion efficiency of 12% and finally load factor of 0.96. Results indicate high concentrations of the resource is constrained to areas of thicker granite bodies and the total area of the resource was 6019 km^2. The areal coverage corresponds to the total resource to a depth of 7 km. The total heat in place available for all uses was determined as 8170 EJ. This corresponds to a recoverable resource of 163 EJ and a technical potential of 249 GW_{th}. There is a significant technical potential as it was assumed that most of the energy can be used with a much higher efficiency in transmission in contrast to that from electricity generation. There is a recorded 5301 EJ of heat in place within the granite at grades high enough for power generation, this translates into a likely recoverable resource of 106 EJ and technical potential over a 30-year lifetime of 14 GW_e (Fig. 6). It should also be noted there could be cascade systems (i.e., electricity generation, followed by district heat network and balneology), which would allow a greater potential of thermal power.

4.2. Probabilistic assessment

A probabilistic assessment was also undertaken to investigate the uncertainty associated to different parametric constraints. MATLAB by MathWorks was used to run over 10,000 simulations which can provide different estimations of the resource, with P10, P50, P90 corresponding to high, medium and low probability estimations (Table 3). For the total heat in place the P50 estimates (Table 3) were elevated in contrast to both deterministic scenarios modelled for total heat in place and that available for electricity generation (Table 2). The reason for this elevation is based on the parameter used for rock density in the deterministic models which is to the lower end of values, but a uniform PDF was applied.

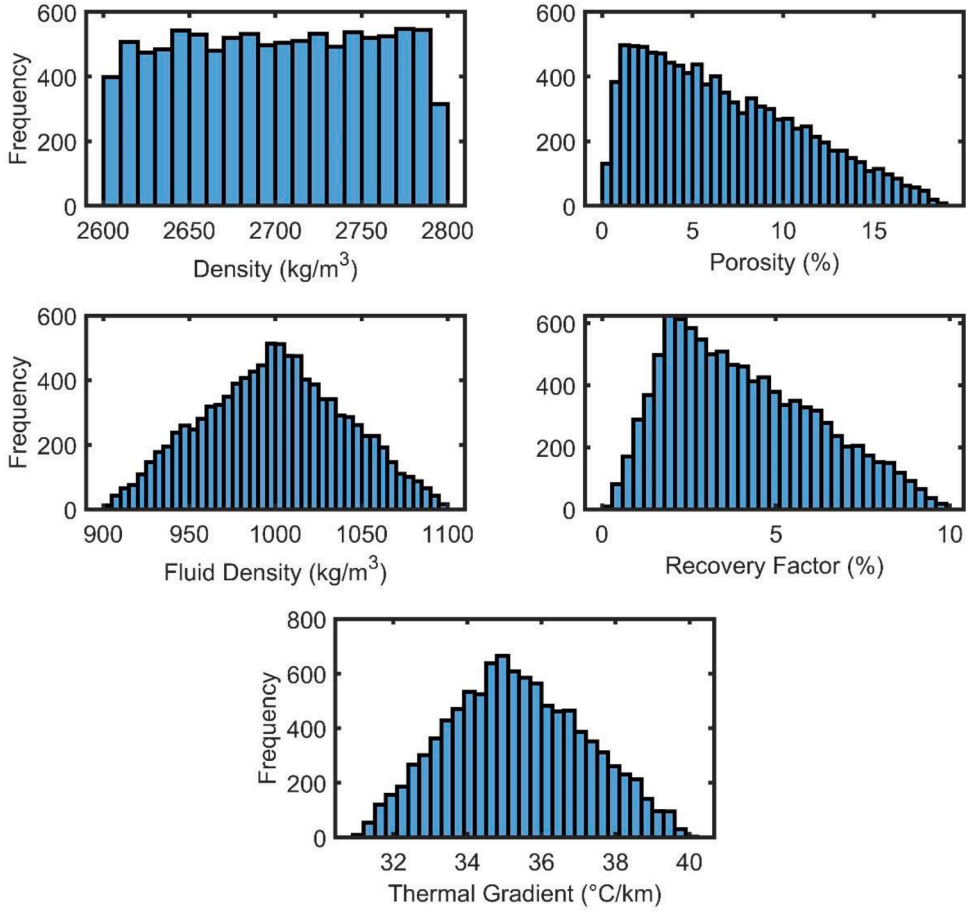

Fig. 4. Distribution Frequency of modelled parameters for total heat use evaluation.

When considering the conventional (P90-P50-P10) probability levels, there is a similar difference between each probability level of just over 800 EJ for the total heat in place. This was also reflected in the increase of recoverable heat (by just over 240 EJ) and just over 400 GW_{th} for the technical potential. The P50 estimates were recorded as 8988 EJ for the total heat in place, 366 EJ for recoverable heat, and a technical potential of 556 GW_{th}. The total heat in place corresponds to 2497 PWh or 1.49 EJ/km^2 (Fig. 7).

The simulations were undertaken for electricity generation only, using a resource cut-off of 100 °C (i.e., using heat in place grid blocks over this temperature only). All values for heat in place, recoverable heat and technical potential were significantly lower. For P50 estimates the heat in place, recoverable heat and technical potential were 5784 EJ, 234 EJ and 31 GW_e, respectively. This corresponds to heat in place of 1607 PWh or 0.96 EJ/km^2 (Fig. 8).

4.3. Most influential parameters

A sensitivity analysis was conducted to assess the significance of input variables in resource assessment calculations using the deterministic method. This analysis employed a one-variable-at-a-time approach, wherein a single variable is altered within its range (using the minimum and maximum values in Table 1, while the thickness was varied using minimum and maximum cut offs for the base of the model of 6 and 8 km, respectively) while holding other variables at their most likely values. The resource base was computed at each step, and tornado charts were generated to evaluate the impact of each input variable. Fig. 9 displays tornado charts for both utilization options. Bar sizes on these charts indicate the swing value, representing the extent of impact. Across all scenarios, reservoir temperature (i.e., as a function of geothermal gradient), thickness, and recovery factor were the most important factors in determining the technical potential, while rock and fluid density, porosity show limited significance. The biggest difference was observed for the recovery factor which resulted in an increase in thermal power to 1243 GW_{th} and for electricity generation to 70 GW_e.

4.4. Evaluating carbon savings

The sustainability attribute of the discussed system is examined in terms of saved annual CO_2 amount by employing geothermal energy rather than fossil fuels, such as natural gas. Results are presented in Table 4, highlighting significant increases in carbon savings with increasing probability levels.

5. Discussion

5.1. Influence of parameters on the resource base

A series of parameters were varied within this work to understand their impact on the total heat in place, recoverable heat and also technical potential of the system. Increased temperature gradients, densities (both fluid and rock), and porosity result in more energy within the system and a greater geothermal potential. In contrast, lower recovery factors result in a reduced recoverable resource and technical potential. However, out of all the parameters simulated the most influential parameter is batholith thickness. If a *minimum* batholith thickness of 10 km, derived by 3D gravity inversion methods (Watts et al., 2024) was adopted the resource could be greater. The 7 km cut-off depth applied in this study could also be extended as drilling capabilities and technologies improve. There are also further uncertainties between the two

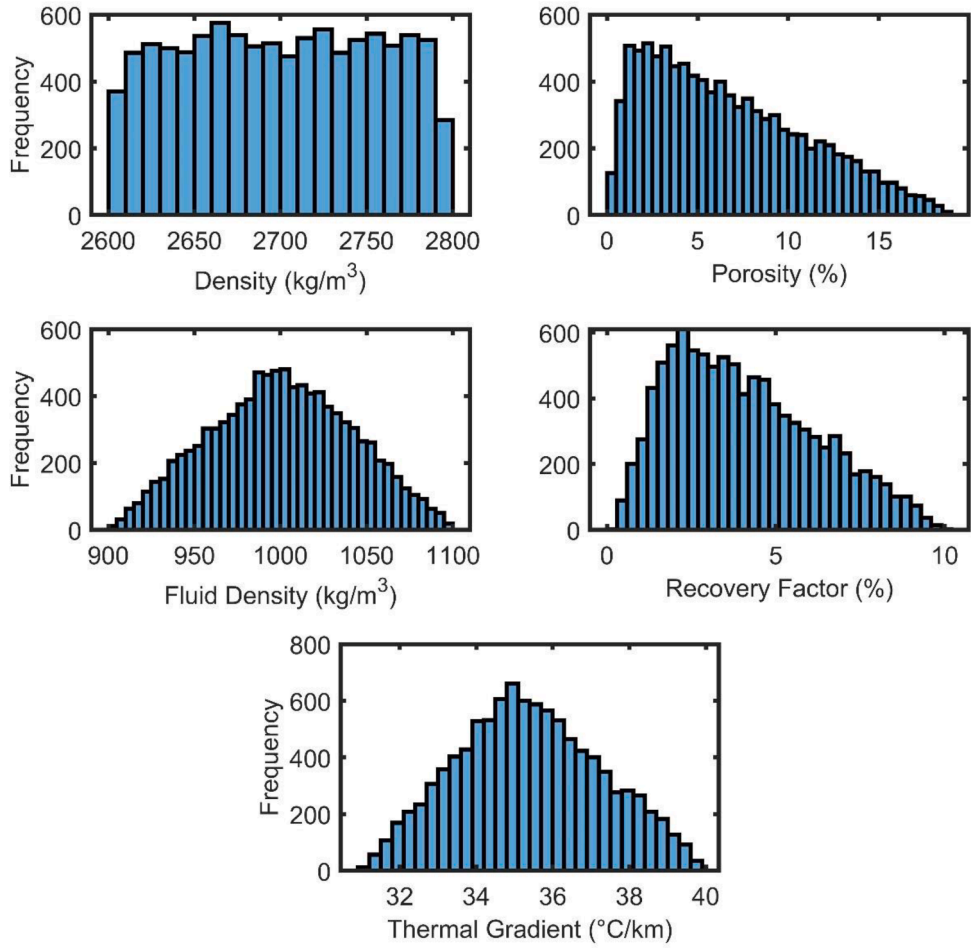

Fig. 5. Distribution Frequency of modelled parameters for electricity generation evaluation.

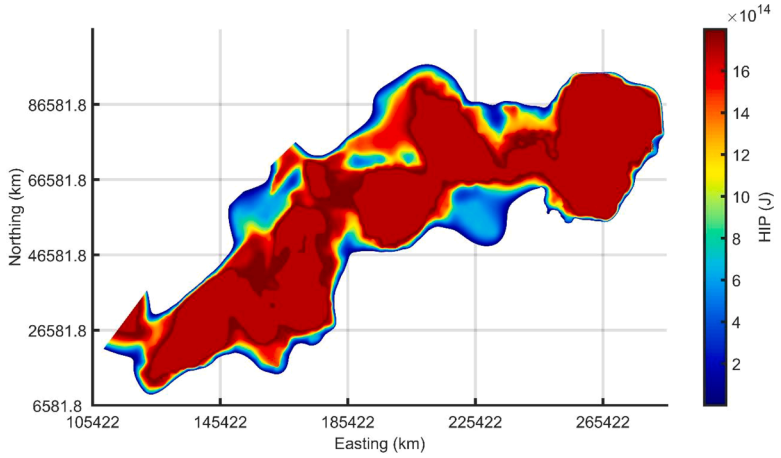

Fig. 6. Heat in Place for the Cornubian batholith available for electricity generation. Derived from Lithoframe data surfaces – Filled_TopGranite and Top-Granite_CHPM_40 m scale BGS Digital Data under Licence No. 2023/108 British Geological Survey © and Database Right UKRI. All rights reserved.

Table 2
Geothermal potential assessment of heat in place.

Parameter	HIP (EJ)	Recoverable Heat (EJ)	Technical Potential (GW)
Total	8170	163	249
Electricity Generation	5301	106	14

methods parametric inputs, such as the rejection temperature and variance in load factors and efficiency. These could impact the overall results.

Future work could look to refine the regional temperature model through static modelling to incorporate variable heat flow (e.g., see Howell et al., 2021). It is also likely that areas near the major plutons with natural fractures, with priority given to Land's End, Carnmenellis and St Austell as they have the highest granite-average temperatures at 5

Table 3
Geothermal potential assessment of heat in place for electricity generation.

Parameter	HIP (EJ)			Recoverable Heat (EJ)			Technical Potential (GW)		
	P90	P50	P10	P90	P50	P10	P90	P50	P10
Total	8167	8988	9824	122	366	614	187	556	938
Electricity Generation	5066	5784	6502	73	234	395	9.5	31	52

Table 4
Results of saved CO_2 amount calculated for stochastic geothermal potential assessment values.

Parameter	P90	P50	P10
Total Carbon Saving (Mt)	319.5	949.9	1602.5
Carbon Saving from Electricity Generation only (Mt)	16.2	105.9	177.7

km depth (Beamish and Busby, 2016), should be targeted for future development.

5.2. Comparison to previous resource estimates

Past work on the Cornubian Batholith has provided a range of estimates for the geothermal potential using deterministic methods. Downing and Gray (1986) conducted a review of the national accessible resource base, investigating the granites within the Southwest, highlighting the heat in place between the 100 °C isotherm and 7 km depth cut-off to be 19,245 EJ. The resource estimate in this study is far higher than that, possibly due to poorer geometrical constraints with the area of the Batholith estimated to be 12,700 km ^{2} by Downing and Gray (1986). The area directly feeds into the bulk volume used to determine heat in place in Eq. (1). Busby and Terrington (2017) also provided a national study into the potential for Enhanced Geothermal Systems, suggesting that the technical potential for the Southwest was c. 28 GW_e. This is similar to that of our study; however, it does include all rocks that could be used (including basement) between 3.5 km and 6.5 km. They also used a slightly higher recovery factor. A report by Jackson (2012) predicted 1100 EJ of heat in place, a technical potential of 13 GW_{th} for total thermal energy and a technical potential of 4 GW_e for electricity. The reason that this study was far lower is because they utilised a smaller area of rock, and higher return temperature. Thus, they predicted lower energy potential. In this study, past work has been built upon, by using new data, a newly digitised geometrical surface to constrains the granite and Monte Carlo Simulations to define uncertainty. At present, there is an annual demand for heating of 463 TWh (BEIS, 2021), thus the Cornubian Batholith P50 estimate of 2497 PWh highlights the significant opportunity for decarbonisation of the heating sector (Table 3).

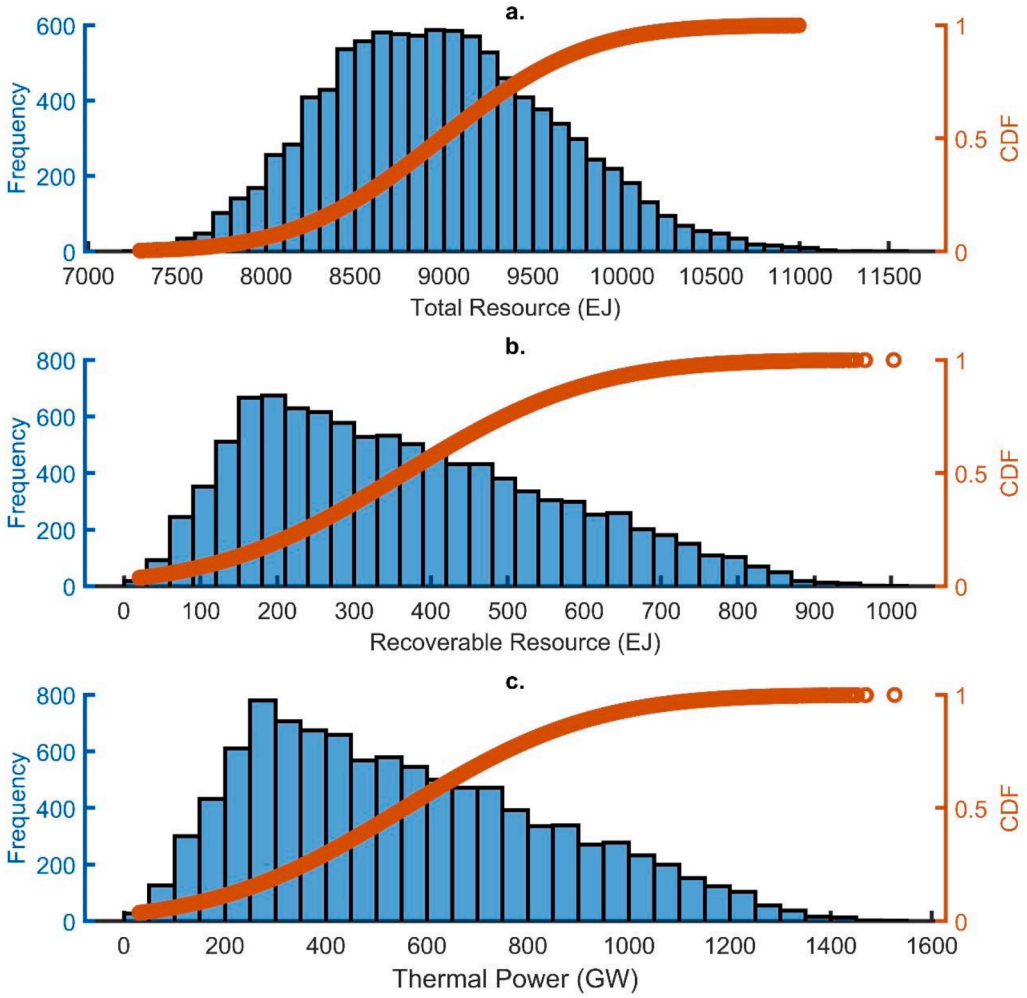

Fig. 7. Cumulative distribution function (red) and distribution frequency of calculated geothermal resource for total heat use evaluation.

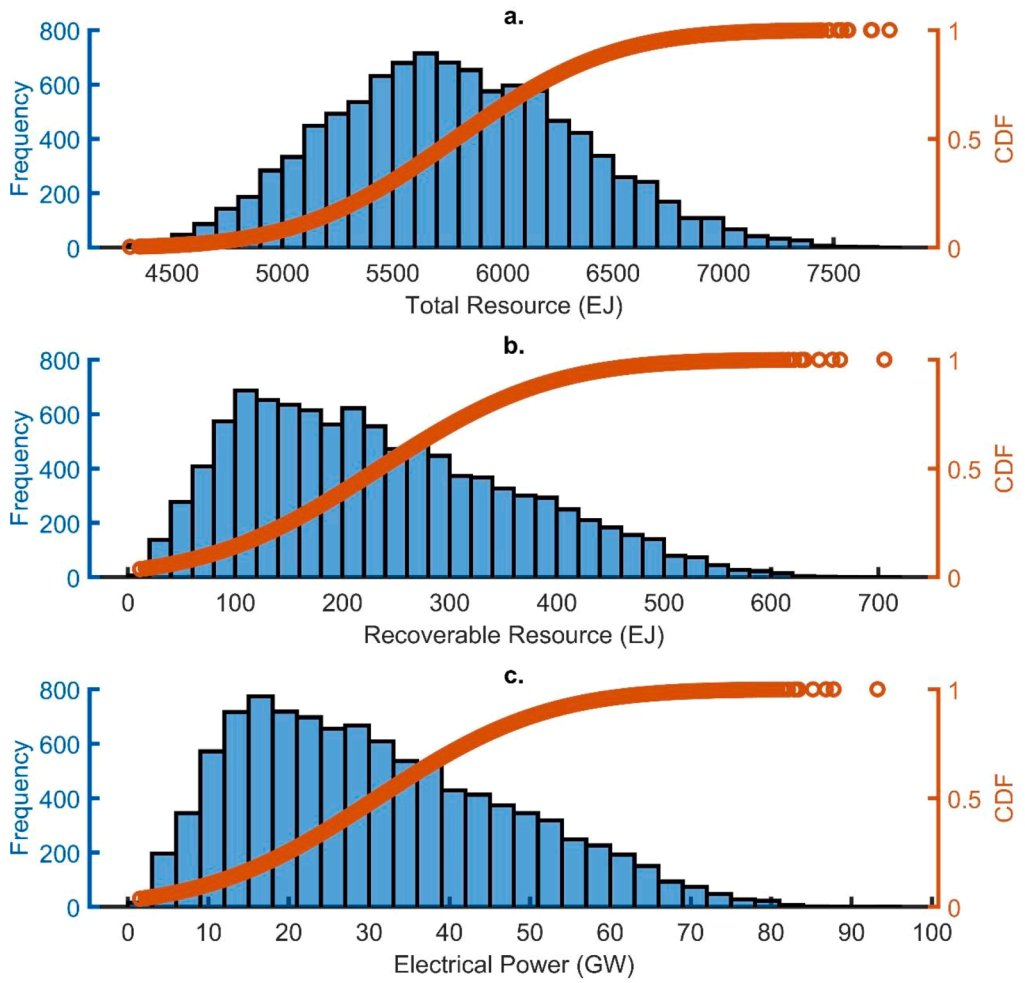

Fig. 8. Cumulative distribution function (red) and distribution frequency of calculated geothermal resource for electricity generation evaluation.

6. Conclusions

This paper provides a refined geothermal resource potential estimate for the Cornubian Batholith using both deterministic and probabilistic methods. New data allowed for improved constraints when utilising the heat in place volumetric method for the resource calculation; this included new petrophysical data and digitised geometrical surfaces for the granite. Within the probabilistic approach 10,000 Monte Carlo Simulations were performed to help to determine uncertainty of the total heat in place, recoverable resource and technical potential. The key conclusions were:

- Deterministic estimations of the resource suggest 8170 EJ of heat could be trapped in place, 163 EJ could be recovered, and the technical potential is 249 GW_{th}. When considering the potential for electricity generation this could be far lower at 5301 EJ, 106 EJ and 14 GW_e, respectively.
- Probabilistic values for the P50 scenario are slightly elevated in contrast the deterministic. This is due to lower bulk densities used for the deterministic than the P50 estimate for probabilistic simulations.
- According to P90 estimates, it is feasible to generate 23,086 times the UK's present installed total capacity: 8.1 MW_{th} (Abesser and Jans-Singh, 2022).
- This study is of regional significance for the granites in Cornwall and Devon, where there has been strong interest in developing the granites. It employs refined data assumptions based on geometrical data (i.e., the surface of the granite, data at depth at the United Downs Project, and from field studies) to improve the resource estimation of heat in place.
- Sensitivity analysis showed that the reservoir temperature, thickness, porosity and recovery factor are the inputs that have greatest impact on accessible resource base and the recoverable heat energy outputs.
- By using geothermal resources rather than natural gas to generate 9.5 GW_e, the annual amount of CO_2 saved is 16.2 Mt and to generate 187 GW_{th}, the annual amount of CO_2 saved is 319.5 Mt.
- Future work could look to develop a full regional 3D heat flow and temperature model for Cornwall and Devon based upon the new data. This could also include modelling of advective flow through fractures, and the incorporation of hydraulic properties. Favourability mapping would also benefit to highlight the most suitable areas for development (e.g., Abuzied et al., 2020; Li et al., 2023). Alternative classifications of resources could be investigated, such as the United Nations Framework Classification (e.g., UNFC, 2019). Finally, transient modelling of the reservoir (e.g., Mahmoodpour et al., 2022a,b) and wellbores (e.g., Brown and Falcone, 2024) would enable a prediction of the system's ability to meet end-user demand in future prospective locations in the region.

Funding

The work is conducted as part of the MEET project that has received funding from the European Union's Horizon 2020 research and innovation programme under grant agreement No 792037.

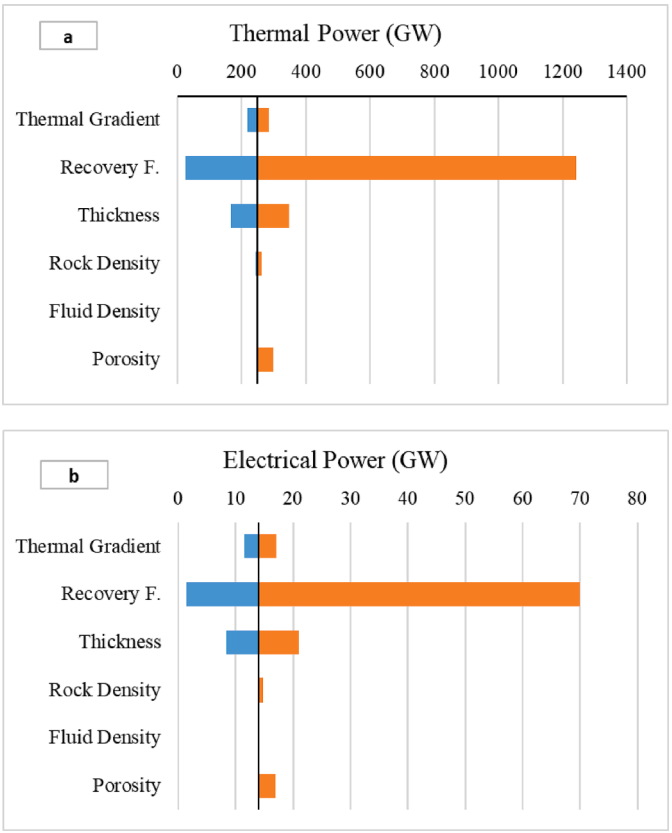

Fig. 9. Tornado charts that show the sensitivity to input parameters: a direct utilization, b indirect utilization. Note that the thickness was based on a decrease and increase of the depth of the base of the granite to 6 and 8 km, respectively.

CRediT authorship contribution statement

Aysegul Turan: Writing – original draft, Visualization, Validation, Methodology, Investigation, Formal analysis, Conceptualization. **Christopher S Brown:** Writing – original draft, Visualization, Validation, Methodology. **Robin Shail:** Writing – review & editing, Visualization. **Ingo Sass:** Writing – review & editing, Supervision, Project administration, Funding acquisition.

Declaration of competing interest

The authors declare that they have no known competing financial interests or personal relationships that could have appeared to influence the work reported in this paper.

Data availability

Data are available online at https://tudatalib.ulb.tu-darmstadt.de/handle/tudatalib/4127

Acknowledgments

This manuscript was prepared as a contribution to the PhD thesis (Group of Geothermal Science and Technology, Institute of Applied Geosciences, Technische Universität Darmstadt) of Aysegul Turan. The authors would also like to thank three anonymous reviewers and editor for their constructive feedback which has significantly improved the paper.

Appendix

Table A1
Grain density, bulk density, porosity, thermal conductivity, thermal diffusivity and specific heat capacity values are summarized here. For coloured copies, outcrop analogue samples (*Turan et al. 2024*) are presented in black, drill cuttings (*Turan et al. 2024*) in blue, *sidewall cores (Stark* et al. *2021)* in italics with red colour in the table. The data publication associated with the parameterisation in this study (*Turan et al., 2024*) contains the raw data of the parameters (grain density and bulk density for the calculation of porosity, thermal conductivity and thermal diffusivity for the calculation of specific heat capacity).

Petrophysical Properties	Min	Max	Average	Median	Number	Standard deviation	Quartile 25%	Quartile 75%
Grain density [kg m^{-3}]	2603	2796	2660	2650	203	38	2639	2662
Grain density [kg m^{-3}]	*2651*	*2777*	*2693*	*2691*	*44*	*26*	*2674*	*2705*
Grain density [kg m^{-3}]	*2642*	*2799*	*2688*	*2673*	*6*	*56*	*2664*	*2681*
Bulk density [kg m^{-3}]	2160	2798	2592	2613	206	74	2562	2634
Bulk density [kg m^{-3}]	*2578*	*2823*	*2689*	*2676*	*6*	*92*	*2616*	*2746*
Porosity [%]	0,03	19,02	2,25	1,05	187,00	2,54	1,00	2,53
Porosity [%]	*0,07*	*2,96*	*1,18*	*0,52*	*3,00*	*1,56*	*0,29*	*1,74*
Thermal conductivity [W m^{-1} K^{-1}]	1,23	5,24	2,79	2,79	195,00	0,56	2,49	2,97
Thermal conductivity [W m^{-1} K^{-1}]	*2,19*	*2,69*	*2,39*	*2,31*	*3,00*	*0,26*	*2,25*	*2,50*
Thermal diffusivity [$\times 10^{-6}$ m^2 $s-1$]	0,76	3,03	1,40	1,36	210,00	0,34	1,20	1,49
Thermal diffusivity [$\times 10^{-6}$ m^2 s^{-1}]	*0,92*	*1,57*	*1,22*	*1,09*	*3,00*	*0,31*	*1,05*	*1,33*
Specific heat capacity (J·kg^{-1}·K^{-1})	475	1066	777	773	148	82	735	827
Specific heat capacity (J·kg^{-1}·K^{-1})	*647*	*816*	*742*	*762*	*3*	*86*	*705*	*789*

Supplementary Materials: Geochemical, petrophysical and petrographical dataset of the fractured Variscan granites of the Cornubian Batholith, SW United Kingdom are available online at https://tudatalib.ulb.tu-darmstadt.de/handle/tudatalib/4127.

Petrophysical and petrological characterization of outcrop analogue samples before and after acidification, chemical characterization of used acids after autoclave experiments, permeability change during Core Floodings Tests are available online at https://tudatalib.ulb.tu-darmstadt.de/handle/tudatalib/2925.

General characterization and results of lab-scale chemical stimulation of side wall cores of the United Downs Deep Geothermal Power Project, Cornwall are available online at https://tudatalib.ulb.tu-darmstadt.de/handle/tudatalib/2926.2.

References

Abesser, C., Jans-Singh, M., 2021. United Kingdom Country Report. July 2022.

Abesser, C., Gonzalez Quiros, A. and Boddy, J., 2023a. The case for deep geothermal energy-unlocking investment at scale in the UK: a deep geothermal energy white paper: detailed report.

Abesser, C., González Quirós, A., Curtis, R., Raine, R., Claridge, H., 2023b. Geothermal energy use, country update for United Kingdom. In: Proceedings of the World Geothermal Congress. Beijing, China.

Abuzied, S.M., Kaiser, M.F., Shendi, E.A.H., Abdel-Fattah, M.I., 2020. Multi-criteria decision support for geothermal resources exploration based on remote sensing, GIS and geophysical techniques along the Gulf of Suez coastal area, Egypt. Geothermics 88, 101893.

Alimonti, C., Soldo, E., Scrocca, D., 2021. Looking forward to a decarbonized era: geothermal potential assessment for oil & gas fields in Italy. Geothermics 93, 102070.

Arkan, S., Parlaktuna, M., 2005. In: Resource Assessment of Balçova Geothermal Field Proceedings World Geothermal Congress 2005, Antalya, Turkey, 24-29 April 2005.

Avşar, Ö., 2011. PhD thesis. Ankara/Middle East Technical University, Ankara.

Barcelona, H., Senger, M., Yagupsky, D., 2021. Resource assessment of the Copahue geothermal field. Geothermics 90, 101987.

Barker, J.A., Downing, R.A., Gray, D.A., Findlay, J., Kellaway, G.A., Parker, R.H., Rollin, K.E., 2000. Hydrogeothermal studies in the United Kingdom. Q. J. Eng. Geol. Hydrogeol. 33 (1), 41–58.

Batchelor, A.S., 1982. Stimulation of a Hot Dry Rock Geothermal Reservoir in the Cornubian granite, England (No. SGP-TR-60; CONF-821214-34). Camborne School of Mines Geothermal Energy Project, Cornwall, England.

Batchelor, T., Curtis, R., Jonathan, B., 2020. Geothermal Energy Use, Country update for United Kingdom. In: Proceedings of World Geothermal Congress 2020. Reykjavik, Iceland. April 26 - May 2.

Batzle, M., Wang, Z., 1992. Seismic properties of pore fluids. Geophysics 57 (11), 1396–1408.

Beamish, D., Busby, J., 2016. The Cornubian geothermal province: heat production and flow in SW England: estimates from boreholes and airborne gamma-ray measurements. Geotherm. Energy 4 (1), 1–25.

BEIS (Department for Business, Energy and Climate Change), 2019. UK becomes first major economy to pass net zero emissions law. Press release. https://www.gov.uk/government/news/uk-becomes-first-major-economy-to-pass-net-zero-emissions-law (27th June 2019) (Accessed 13 December 2023).

BEIS, 2021. Opportunity areas for district heating networks in the UK. National Comprehensive Assessment of the potential for efficient heating and cooling. Available from: https://assets.publishing.service.gov.uk/government/uploads/system/uploads/attachment_data/file/1015585/opps_for_dhnnca_hc.pdf.

Bott, M.H.P., Day, A.A., Masson-Smith, D., 1958. The geological interpretation of gravity and magnetic surveys in Devon and Cornwall. Philosoph. Transact. Roy. Soc. Lond. Ser. A, Math. Phys. Sci. 251, 161–191.

Breede, K., Dzebisashvili, K., Falcone, G., 2015. Overcoming challenges in the classification of deep geothermal potential. Geotherm. Energy Sci. 3 (1), 19–39. https://doi.org/10.5194/gtes-3-19-2015.

Brooks, M., Doody, J.J., Al-Rawi, F.R.J., 1984. Major crustal reflectors beneath SW England. J. Geol. Soc. 141 (1), 97–103.

Brown, C.S., 2022. Regional geothermal resource assessment of hot dry rocks in Northern England using 3D geological and thermal models. Geothermics 105, 102503.

Brown, C.S., 2023. Revisiting the Deep Geothermal Potential of the Cheshire Basin, UK. Energies 16 (3), 1410.

Brown, C.S., Howell, L., 2023. Unlocking deep geothermal energy in the UK using borehole heat exchangers. Geol. Today 39 (2), 67–71.

Brown, C.S., Doran, H., Kolo, I., Banks, D., Falcone, G., 2023. Investigating the Influence of Groundwater Flow and Charge Cycle Duration on Deep Borehole Heat Exchangers for Heat Extraction and Borehole Thermal Energy Storage. Energies 16 (6), 2677.

Brown, C.S., Kolo, I., Banks, D., Falcone, G., 2024. Comparison of the thermal and hydraulic performance of single U-tube, double U-tube and coaxial medium-to-deep borehole heat exchangers. Geothermics 117, 102888.

Brown, C.S., Falcone, G., 2024. Investigating heat transmission in a wellbore for low-temperature, open-loop geothermal systems. Therm. Sci. Eng. Progr., 102352

Busby, J., 2014. Geothermal energy in sedimentary basins in the UK. Hydrogeol. J. 22 (1), 129–141.

Busby, J., Terrington, R., 2017. Assessment of the resource base for engineered geothermal systems in Great Britain. Geotherm. Energy 5, 1–18.

Chen, Y., Clark, A., Farrar, E., Wasteneys, H., Hodgson, M., Bromley, A., 1993. Diachronous and independent histories of plutonism and mineralization in the Cornubian Batholith, southwest England. J. Geol. Soc. Lond. (150), 1183–1191.

Çengel, Y.A., 2020. Power generation potential of liquified natural gas regasification terminals. Int. J. Energy Res. 44, 3241–3252. https://doi.org/10.1002/er.5116.

Dalby, C.J., 2023. Doctoral dissertation. University of Exeter.

Department for Energy Security and Net Zero, Prime Minister's Office, and Department for Business, Energy & Industrial Strategy. (2022, April). British Energy Security Strategy. URL: https://assets.publishing.service.gov.uk/government/uploads/system/uploads/attachment_data/file/1069969/british-energy-security-strategy-web-accessible.pdf.

Dearman, W.R., 1963. Wrench-faulting in Cornwall and south Devon. Proc. Geol. Assoc. 74 (3), 265–287. https://doi.org/10.1016/S0016-7878(63)80023-1.

Department for Business, Energy, and Industrial Strategy, 2019. 2018 UK Greenhouse Gas Emissions, Provisional Figures – Statistical Release. National Statistics. https://assets.publishing.service.gov.uk/media/5c9ce8b240f0b633f24d054a/2018-provisional-emissions-statistics-report.pdf.

Downing, R.A., Gray, D.A., 1986. Geothermal Energy: the Potential in the United Kingdom. British Geological Survey. HMSO, London.

Eswara, A.K., Misra, S.C., Ramesh, U.S., 2013. Introduction to natural gas: a comparative study of its storage, fuel costs and emissions for a harbor tug. In: Proceedings of the Annual Meeting of Society of Naval Architects & Marine Engineers (SNAME). Bellevue, WA, USA, pp. 1–21, 8 November.

Edmunds, W.M., Andrews, J.N., Burgess, W.G., Kay, R.L.F., Lee, D.J., 1984. The evolution of saline and thermal groundwaters in the Carnmenellis granite. Miner. Mag. 48, 407–424.

Garg, S.K., Combs, J., 2015. A reformulation of USGS volumetric "heat in place" resource estimation method. Geothermics 55, 150–158. https://doi.org/10.1016/j.geothermics.2015.02.004.

Gluyas, J.G., Adams, C.A., Busby, J.P., Craig, J., Hirst, C., Manning, D.A.C., McCay, A., Narayan, N.S., Robinson, H.L., Watson, S.M., Westaway, R., 2018. Keeping warm: a review of deep geothermal potential of the UK. Proceedings of the Institution of Mechanical Engineers. Part A: J. Power Energy 232 (1), 115–126.

Grant, M.A., 2016. Physical performance indicators for HDR/EGS projects. Geothermics 63, 2–4.

Hache, E., 2018. Do renewable energies improve energy security in the long run? Int. Econ. 156, 127–135.

Howell, L., Brown, C.S., Egan, S.S., 2021. Deep geothermal energy in northern England: insights from 3D finite difference temperature modelling. Comput. Geosci. 147, 104661.

Huebert, J., 2023. British Geological Survey Open Report, p. 48. OR/23/031.

Intergovernmental Panel on Climate Change. (2021). Climate Change 2021: the Physical Science Basis. Retrieved from https://www.ipcc.ch/report/ar6/wg1/.

Jones, D.J., Randles, T., Kearsey, T., Pharaoh, T.C., Newell, A., 2023. Deep geothermal resource assessment of early carboniferous limestones for Central and Southern Great Britain. Geothermics 109, 102649.

Korkmaz, E.D., Serpen, U., Satman, A., 2014. Geothermal boom in Turkey: growth in identified capacities and potentials. Renew. Energy 68, 314–325. https://doi.org/10.1016/j.renene.2014.01.044.

Ledingham, P., Cotton, L. and Law, R., 2019. The united downs deep geothermal power project.

Leveridge, B.E., Hartley, A.J, 2006. The Variscan Orogeny: the development and deformation of Devonian/Carboniferous basins in SW England and South Wales. In: Brenchley, P.J., Rawson, P.F. (Eds.), The Geology of England and Wales. Geological Society of London, pp. 225–255.

Li, X., Huang, C., Chen, W., Li, Y., Han, J., Wang, X., Bai, X., Yin, Z., Li, X., Hou, P., Tong, J., 2023. GIS model for geothermal advantageous target selection. Sci. Rep. 13 (1), 6024.

Mahmoodpour, S., Singh, M., Obaje, C., Tangirala, S.K., Reinecker, J., Bär, K., Sass, I., 2022a. Hydrothermal numerical simulation of injection operations at United Downs, Cornwall, UK. Geosciences 12 (8), 296.

Mahmoodpour, S., Singh, M., Turan, A., Bär, K., Sass, I., 2022b. Simulations and global sensitivity analysis of the thermo-hydraulic-mechanical processes in a fractured geothermal reservoir. Energy 247, 123511.

Met Office. (n.d.). UK Climate Averages. Retrieved November 14, 2023, from https://www.metoffice.gov.uk/research/climate/maps-and-data/uk-climate-averages/gchc0ssk0.

Meşin, V., Karakaya, A., 2023. Contribution of geothermal resources that could be used in district heating system to Türkiye economy and analysis in terms of carbon emissions. J. Polytechn. 26 (1), 345–355.

Micromeritics, 1998. GeoPyc 1360, V3., Part 136-42801-01. Micromeritics GmbH, Munich, Germany, p. p69.

Micromeritics, 2023. Product Showcase: AccuPyc II 1340 Specification Sheet. Retrieved from. https://www.micromeritics.com/downloads/Brochures/English/AccuPyc.pdf.

Muffler, L J.P., 1978. Assessment of Geothermal Resources of the United States. United States. https://doi.org/10.2172/687040.

Muffler, P., Cataldi, R., 1978. Methods for regional assessment of geothermal resources. Geothermics 7 (2–4), 53–89.

Paulillo, A., Cotton, L., Law, R., Striolo, A., Lettieri, P., 2020. Geothermal energy in the UK: the life-cycle environmental impacts of electricity production from the United Downs Deep Geothermal Power project. J. Clean. Prod. 249, 119410.

Pearson, P.J.G., Watson, J., 2023. The unfolding low-carbon transition in the UK electricity system. Proc. Nat. Acad. Sci. 120 (47), e2206235120 https://doi.org/10.1073/pnas.2206235120.

Reinecker, J., Gutmanis, J., Foxford, A., Cotton, L., Dalby, C., Law, R., 2021. Geothermal exploration and reservoir modelling of the United Downs deep geothermal project, Cornwall (UK). Geothermics 97, 102226.

Sanyal, S.K, 2005. Sustainability and renewability of geothermal power capacity. In: Proceedings of the World Geothermal Congress 2005. Retrieved from. http://www.geothermal-energy.org/pdf/IGAstandard/WGC/2005/0520.pdf.

Shail, R.K., Alexander, A.C., 1997. Late Carboniferous to Triassic reactivation of Variscan basement in the western English Channel: evidence from onshore exposures in south Cornwall. J. Geol. Soc. 154 (1), 163–168.

Shail, R.K., Leveridge, B.E., 2009. The Rhenohercynian passive margin of SW England: development, inversion and extensional reactivation. Comptes Rendus Geosci. 341, 140–155.

Shail, R., Simons, B., 2023. The Cornubian Batholith: post-collisional variscan granites and resources. In: Decrée, S. (Ed.), Metallic Resources 1: Geodynamic Framework and Remarkable Examples in Europe. ISTE-Wiley, London, pp. 143–219.

Simons, B., Shail, R.K., Andersen, J.C.Ø., 2016. The petrogenesis of the Early Permian Variscan granites of the Cornubian Batholith: lower plate post-collisional peraluminous magmatism in the Rhenohercynian Zone of SW England. Lithos 260, 76–94.

Somma, R., Blessent, D., Raymond, J., Constance, M., Cotton, L., Natale, G.D., Fedele, A., Jurado, M.J., Marcia, K., Miranda, M., et al., 2021. Review of recent drilling projects in unconventional geothermal resources at Campi Flegrei Caldera, Cornubian Batholith, and Williston Sedimentary Basin. Energies 14 (3306). https://doi.org/10.3390/en14113306.

Stark, M., Bär, K., Sass, I., 2021. Side Wall Cores of the United Downs Deep Geothermal Power Project, Cornwall: General Characterisation and Results of Lab-Scale Chemical Stimulation of Fractured Granite Reservoir Samples. TU Darmstadt Data Lib. Retrieved from. https://tudatalib.ulb.tu-darmstadt.de/handle/tudatalib/2926.2.

Taylor, G.K., 2007. Pluton shapes in the Cornubian Batholith: new perspectives from gravity modelling. J. Geol. Soc. 164 (3):, 525–528. https://doi.org/10.1144/0016-76492006-104.

Tester, J.W., Anderson, B.J., Batchelor, A.S., Blackwell, D.D., DiPippo, R., Drake, E.M., Garnish, J., Livesay, B., Moore, M.C., Nichols, K., Petty, S., Toksöz, M.N., Veatch, R. W., 2006. The Future of Geothermal energy: Impact of Enhanced Geothermal Systems (EGS) On the United States in the 21st Century. MIT.

Turan, A., Artun, E., Saner, S., 2021. Probabilistic assessment of geothermal resources and their development in Dikili-İzmir region. SN Appl. Sci. 3 (6), 634.

Turan, A., Bär, K., Sass, I., 2024. Geochemical, Petrophysical and Petrographical Dataset of Fractured Variscan granites of the Cornubian Batholith, SW United Kingdom. TU Darmstadt Data Lib. *Retrieved from*. https://tudatalib.ulb.tu-darmstadt.de/handle/tudatalib/.

UNFC, 2019. United Nations framework classification for resources: update 2019. *(ECE ENERGY SERIES No. 61)*.

Watson, S.M., Westaway, R., Falcone, G., 2019. A review of deep geothermal energy and future opportunities in the UK. In: Proc. European Geothermal Congress.

Watts, A.B., Xu, C., Searle, M.P., Jurkowski, C., Shail, R.K., 2024. The Permian Cornubian granite batholith, SW England: part 2: gravity anomalies, structure, and state of isostasy. GSA Bull. https://doi.org/10.1130/B37459.1.

Williams, C.F., 2007. Updated methods for estimating recovery factors for geothermal resources. In: Proceedings of the Thirty-Second Workshop on Geothermal Reservoir Engineering (SGP-TR-183). Stanford University, Stanford, California. January 22-24U.S. Geological Survey.

Willis-Richards, J., Jackson, N.J., 1989. Evolution of the Cornubian Ore Field, Southwest England: Part I. Batholith Modeling and Ore Distribution. Econ. Geol. 84, 1078–1100.

Yamanlar, S., Korkmaz, E.D., Serpen, U., 2020. Assessment of geothermal power potential in Buyuk Menderes Basin, Turkey. Geothermics 88, 101912. https://doi.org/10.1016/j.geothermics.2020.101912.

Yeomans, C.M., Claridge, Hester, Hudson, A.J.L., Shail, R.K., Willems, C., Eyre, M., et al., 2022. A single multi-scale and multi-sourced semi-automated lineament detection technique for detailed structural mapping with applications to geothermal energy exploration. Geolog. Soc. Lond. Collect. https://doi.org/10.6084/m9.figshare.c.6309629.v1.

Younger, P.L., Gluyas, J.G., Stephens, W.E., 2012. Development of deep geothermal energy resources in the UK. Proceed. Instit. Civil Eng.-Energy 165 (1), 19–32.